Molecular studies into Copine-4 function in Retinal Ganglion Cells

Manvi Goel[1,2], Angel M. Aponte[3], Graeme Wistow[4], Tudor C. Badea*[1,5]

[1] Retinal Circuit Development & Genetics Unit, Neurobiology Neurodegeneration & Repair Laboratory, NEI, National Institutes of Health, Bethesda, Maryland 20892

[2] Department of Neuroscience, College of Medicine, The Ohio State University, 333 W 10th Avenue, Columbus, Ohio 43210

[3] Proteomics Core, NHLBI, National Institutes of Health, Bethesda, Maryland 20892

[4] Section on Molecular Structure and Functional Genomics, NEI, National Institutes of Health, Bethesda , Maryland 20892

[5] Research and Development Institute, Faculty of Medicine, Transilvania University of Brasov, Brasov, Romania

* Corresponding author: Tudor C. Badea,

Retinal Circuit Development & Genetics Unit, Building 6, Room 331, 6 Center Drive, Bethesda, MD 20892-0610. / Research and Development Institute, Transilvania University of Brasov, Blvd. Eroilor Nr. 29, Brasov, cod 500036, Romania.

Email: badeatc@mail.nih.gov / badeatc@unitbv.ro

ABSTRACT

The molecular mechanisms underlying morphological diversity in retinal cell types are poorly understood. We have previously reported that several members of the Copine family of Ca-dependent membrane adaptors are expressed in Retinal Ganglion Cells (RGCs) and transcriptionally regulated by Brn3 transcription factors. Several Copines are enriched in the retina and their over-expression leads to morphological changes reminiscent of neurite formation in HEK293 cells. However, the role of Copines in the retina is largely unknown. Here we focus on Cpne4, a Copine whose expression is restricted to RGCs. Over-expression of Cpne4 in RGCs in vivo led to formation of large varicosities on the dendrites but did not otherwise visibly affect dendrite or axon formation. Protein interactions studies using yeast two hybrid analysis from whole retina cDNA revealed two Cpne4 interacting proteins - HCFC1 and Morn2. Mass Spectrometry analysis of retina lysate pulled down using Cpne4 or its vonWillebrand A (vWA) domain identified a further 207 interacting proteins. Gene Ontology (GO) analysis of Cpne4 interactors suggests its involvement in several metabolic and signaling pathways, including processes related to vesicle trafficking, intracellular membrane bound organelles, and plasma membrane associated structures, including neurites. We conclude that, consistent with its domain structure, Cpne4 may be involved in assembly and trafficking of several membrane associated cell compartments.

48 **1. INTRODUCTION**

49 RGCs in the retina transmit visual signals received by photoreceptors to the brain for
50 processing visual inputs. Different RGC sub-types are responsible for computing different
51 aspects of the visual stimuli. The combinatorial expression of transcription factors in different
52 RGC sub-types regulates cell specific morphologies and physiology by controlling molecules
53 involved in the development of dendrite/axon morphology, synapse formation and function (1,2).

54 How cell-specific morphologies develop in the retina is not well understood. One likely
55 mechanism is that transcription factors encode specific morphological features via adhesion
56 molecules or cytoskeletal elements they regulate. For example, Tbr1 regulates cell adhesion
57 molecules Cdh8 and Sorcs3 resulting in dendritic stratification of J-RGCs in the Off sublamina
58 (3). Other such molecules might be responsible for cell specific morphologies in other RGC
59 types. Copines are a family of such candidate cell morphology determinants, regulated by Brn3
60 transcription factors. Copines consist of two C2 domains (C2A and C2B) and a vWA domain
61 (4,5). The Copine C2 domains are similar to those found in a variety of vesicular traffic proteins
62 such as Synaptotagmins, Munc18, Rabphilin3A and Doc2, and have been involved in calcium
63 dependent binding to cell membranes (6). vWA domains are typically found extracellularly in
64 several proteins (e.g. integrins) and are involved in protein-protein interactions (7). However
65 Copines (and their vWA domain) are intracellular proteins that interact transiently with the inner
66 leaflet of the plasma membrane.

67 There are nine Copines in mammals- Cpne1- 9 (4,8–10). Of these, Cpne1, 2 and 3 are
68 expressed ubiquitously. Cpne4, 5, 6, 7, 8 and 9 are enriched in neurons. Cpne5 and 8 are also
69 expressed in other tissues such as kidneys, lungs, testes, mammary glands (11,12).

70 Copines are conserved across several species. They have previously been shown to be
71 important in a variety of cellular functions. Copines are involved in myofilament stability in C.
72 elegans and plant growth in Arabidopsis (13,14). Copines are also involved in cytokinesis and
73 contractile vacuole function by regulating cAMP signaling in Dictyostelium (15). Copine has
74 also been shown to interact with actin filaments to regulate chemotaxis and adhesion in
75 Dictyostelium (16).
76 In the nervous system, Copines were first seen to be localized in hippocampus and
77 olfactory bulb neurons in mouse brain (10,17). Cpne6 is expressed in the hippocampus and is
78 required for regulating the spine morphology during long term potentiation in hippocampus by
79 regulating the Rac-LIMK-Cofilin and BDNF-TrkB pathways (18,19). Cpne1 has been previously
80 seen to be upregulated during development and is required for hippocampal progenitor cell
81 differentiation into neurons (20,21). Cpne7 is expressed in sublaterodorsal nucleus in pontine
82 segmental area and is required for REM sleep (22).
83 In the retina, we have previously reported that Cpne4, 5, 6 and 9 are enriched in the inner
84 retina and they are regulated by Brn3b and Brn3a (1,23). Whereas Cpne5, 6 and 9 were
85 expressed in most of the GCL as well as INL, Cpne4 is the only Copine specifically expressed in
86 RGCs (with the exception of one INL amacrine cell type) (23). Using over-expression studies in
87 HEK293 cells, we found that Copines can significantly alter cell morphology, inducing
88 elongated membrane processes similar to neurites. In the current study, we further explore the
89 effects of Cpne4 expression in RGCs and study its protein interactions using yeast two hybrid
90 analysis and Mass Spectrometry, to identify its cell biological functions and role in RGCs.
91
92 **2. MATERIALS AND METHODS**

93 **2.1 Transfection in HEK293-Cre cells**

94 The cDNA for full length Cpne4, two C2 domain or vWA domain were cloned into
95 pAAV-FLEX-HA-T2A-meGFP plasmid vector (Fig.1A). The cDNA is in frame with 3XHA (3
96 tandem copies of Hemagglutinin antigen tag- 5' TACCCATACGATGTTCCAGATTACGCT 3'
97 or 5' TATCCATATGATGTTCCAGATTATGCT 3') and separated from meGFP (membrane
98 eGFP) by a P2A peptide sequence. The constructs were transfected into HEK293-Cre cells (a
99 kind gift of Dr. Brian Sauer) [1, 23, 62] using Lipofectamine (Invitrogen, Carlsbad, CA). The
100 transfected cells were fixed in 2%PFA after 48 hours and processed for immunofluoroscence as
101 described in section 2.4.

102

103 **2.2 Mouse lines**

104 Adult *Brn3b*$^{KO/KO}$ (or KO) (24) and *Brn3b*$^{W/WT}$ (or WT) littermates were used for
105 immunohistochemistry (IHC). Postnatal day 0 (P0) or P14 *Brn3b*$^{Cre/WT}$ mice were used for AAV1
106 virus infections. Adult wild-type (C57/Bl6 – SV129 mixed background) mice were used for
107 retina pulldowns and mass spectrometry experiments, to determine the protein interactors of
108 Cpne4. All animal procedures were approved by the National Eye Institute (NEI) Animal Care
109 and Use Committee under protocol NEI640.

110

111

112 **2.3 Virus infections in retina**

113 Flex-meGFP-P2A-HA-Cpne4, described in section 2.1, was packaged into AAV1 viruses
114 (henceforth AAV1-Cpne4). Intraocular injections of 0.5 ul (1e9 viral particles/ul) of AAV1-
115 Cpne4 or AAV1-eGFP control virus were done in P0 or P14 Brn3bCre/WT mice eyes using

116 glass capillaries fitted onto a Femtojet device (Eppendorf, Enfield, CT), as previously described.
117 Injections were aimed at the scleral region adjacent to the limbus. Eyes were collected at 2-3
118 months of age and flat-mounted for immunostaining. The eyes were fixed in 4%
119 paraformaldehyde for 15 minutes and retinas were dissected to make a flat mount preparation.
120 The retinas were again fixed for 30 minutes and then washed three times with PBS+ 0.5%
121 Triton-X 100 (PBST). Immunofluorescence was performed as described below.
122

123 **2.4 Immunofluorescence**

124 Brn3b WT and KO sections were co-immunostained to confirm the presence of different
125 interactor proteins identified from yeast two hybrid and mass spectrometry analysis in the retinal
126 ganglion cells. Similar process was followed for immunofluorescence of transfected HEK293
127 cells on coverslips. The sections or cells were incubated with blocking solution- 10% bovine
128 serum albumin (BSA), 10% normal donkey serum (NDS) and 0.5% Triton X 100, for one hour at
129 room temperature. The blocking solution was then replaced with primary antibody solution
130 containing the antibodies at the required concentrations and incubated overnight, at 4^0C. Sections
131 or cells were washed three times with PBST and incubated with the secondary antibody solutions
132 for one hour at room temperature. The sections or cells were washed again with PBST and
133 coverslipped.

134 For staining the AAV1 infected retina flatmounts, the retinas were incubated in blocking
135 solution, overnight at 4^0C. The blocking solution was then replaced with primary antibody
136 solution and retinas incubated for 48 hours at 4^0C. The retinas were then washed three times in
137 PBST, secondary antibody solution was added and retinas were incubated overnight at 4^0C. The
138 retinas were washed again three times with PBST, carefully mounted on glass slides and

139 coverslips were placed. Image acquisition was on either a Axioimager Z2 fitted with an apotome
140 device, or on a LSM 880 confocal microscope (both from Zeiss, White Plains, NY). The images
141 were taken as 1um thick z-stacks and the images were stacked using ImageJ. Colocalization
142 analysis of Copine4-interacting proteins in HEK293 cells was performed using the "Coloc 2"
143 plugin in ImageJ.
144
145 **2.5 Yeast two hybrid**
146 A Gal4 based yeast two hybrid analysis was performed to identify the proteins that
147 interact with Cpne4 vWA domain. An adult mouse retina cDNA library was cloned in pGADT7
148 (carrying a Trp1 selection gene) and transformed in AH109 yeast strain (containing His3, Ade2,
149 lacZ and Mel1 selections; Clontech, BD Biosciences, Pao Alto, CA). Cpne4 vWA domain was
150 cloned into pGBKT7 (carrying Leu2 selection gene) and transformed in to competent Y187 yeast
151 strain (lacZ and Mel1 selection). The yeast mating experiment was performed as per the Two-
152 hybrid library screening protocol for yeast mating (Clontech). Briefly, one colony of Y187
153 transformed with pGBKT7+ Cpne4 vWAdomain was inoculated in 50 ml of Tryptophan (Trp)
154 selection media and incubated at 30^0C overnight. The following day, the culture media was
155 centrifuged, and the pellet re-suspended in 5ml Trp selection media. 45ml of YPDA media (YPD
156 media supplemented with adenine(Ade)) was added to it. 1ml of cDNA library (titer= 5 x
157 10^7cfu/ml) was thawed in a water bath at room temperature and added to the above and allowed
158 to mate for approximately 24 hours at 30^0C with slow shaking at 50rpm. The next day, the
159 presence of mated, diploid yeast cells was checked under light microscope. The culture was then
160 centrifuged, and the pellet resuspended in 15ml 0.5X YPDA. 300ul aliquots of the entire 15ml
161 mating culture was spread on 15cm quadruple selection agar plates (with selection for Trp,

162 leucine (Leu), Ade and histidine (His) and X-alpha-Gal reporter) and grown for about 5 days at
163 30^0C. Small scale positive and negative control matings were also performed. For the positive
164 control, pGBKT7-53 encoding the p53 protein and pGADT7-T encoding the SV40 large T
165 antigen protein were transformed into Y187 and AH109, respectively. For negative control,
166 empty pGBKT7 and pGADT7, with no gene insertions, were transformed into Y187 and AH109,
167 respectively. For the positive control mating, one colony each from Y187 + pGBKT7-53 and
168 AH109 + pGADT7-T were inoculated in 500ul 2X YPDA and incubated overnight at 30 degrees
169 at 200rpm. Similarly, for the negative control mating, Y187 + empty pGBKT7 and AH109 +
170 pGADT7 were inoculated in 500ul 2X YPDA and incubated overnight at 30 degrees at 200rpm.
171 The following day the control cultures were spread in 1:10, 1:100 and 1:1000 dilutions on
172 separate single (Leu or Trp), double (Leu and Trp) or quadruple selection agar plates and grown
173 for 3-5 days at 30^0C.
174 After 4 days of selection, 241 pale blue colonies were picked for confirmation. They were
175 streaked separately on fresh agar plates with quadruple selection. Six colonies grew into blue
176 colonies after 3-4 days. For both positive and negative controls, the colonies appeared on the
177 single selection and double selection plates. But on the quadruple selection plates, blue colonies
178 appeared only on the positive control and there were no colonies for the negative control.
179 Colony PCR was performed on the six selected colonies, and PCR products were extracted from
180 the gel and Sanger sequenced (Eurofins, Luxembourg). Inserts were identified by BLAST
181 searches against the NCBI mouse transcriptome collection.
182
183 **2.6 Co-immunoprecipitation**

184 HEK293-Cre cells were co-transfected with HA-eGFP-Cpne4-vWAdomain construct
185 (described in section 2.1) and Flag- tagged target protein or protein domain identified from yeast
186 two hybrid analysis. 24 hours after the transfection, the cells were washed three times with 1X
187 PBS. 300ul lysis buffer (50mM Tris-HCl, 150mM NaCl, 0.5% NP40 and 1mM EDTA)
188 containing protease inhibitor (Roche, Basel, Switzerland) and 0.2M PMSF was added to each
189 well and incubated on ice for 15 minutes. The lysate was then collected in 1.5ml tubes and
190 centrifuged at 14000g for 10 minutes to remove any debris. Meanwhile, magnetic beads were
191 washed with 1X PBS and incubated with Flag antibody for 30 minutes, with end-to-end rotation
192 at 4^0C. The beads were again washed with 1X PBS to remove any unbound antibody and the
193 supernatant from the cell lysate was added to it. These were incubated overnight with end-to-end
194 rotation at 4^0C. The next day, the beads were washed four times and PBS + Laemmli buffer
195 (62.5mM Tris-HCl, 2% SDS, 10% glycerol, 5% beta-mercapto-ethanol, bromophenol blue) was
196 added to the beads. The beads were boiled for 5 minutes at 70^0C. The beads were separated on a
197 magnetic rack and the supernatant loaded on a 10% SDS-PAGE gel. The gel was allowed to run
198 until the dye front reached the bottom of the gel. The separated proteins were then transferred to
199 0.2um PVDF membranes and processed further for Western blotting.
200
201 **2.7 GST pulldown from retina**
202 GST tagged Cpne4 protein was synthesized from bacteria as described before (23). GST-
203 Cpne4-vWAdomain and GST proteins were also synthesized similarly. 19 wild-type retinas
204 (C57Bl6 and SV129) were homogenized using a glass homogenizer, in cold lysis buffer (RIPA
205 buffer: 50mM Tris-HCl, 150mM NaCl, 1mM EDTA, Complete protease inhibitor (Millipore
206 Sigma, Burlington, MA; Catalog no. 11697498001)). NP40 was then added to the lysate to a

207 0.5% final concentration. Glutathione- tagged magnetic beads were added to the lysate and
208 incubated at 4 degrees with end-to-end rotation for 2 hours. The magnetic beads were removed,
209 and the lysate centrifuged at 700g for 10 minutes to remove any debris. The lysate was then kept
210 on ice until further process. Equimolar amounts of GST, GST-vWA domain and GST-Cpne4
211 were incubated with glutathione tagged magnetic beads and incubated with end-to-end rotation at
212 4^0C for 2 hours. The supernatant was discarded, and beads washed three times with PBS. Equal
213 volume of cleared retina lysate (600ul each) was added to each of the above three tubes and
214 incubated overnight at 4^0C with end-to-end rotation. The following day, the supernatant was
215 discarded, and the beads were washed four times with PBS. 30ul of glutathione elution buffer
216 was added to each of the tubes and incubated at room temperature for 10 minutes with end-to-
217 end rotation. Laemmli buffer was added and the samples boiled at 70^0C for 5 minutes. The beads
218 were separated, and the samples loaded onto 4-15% gradient SDS-PAGE gels. The samples were
219 allowed to run on the gel until the dye front reached the bottom and proteins were visualized
220 using Coomassie blue staining. Full lanes were cut out of the gel for each of the three samples,
221 cut into smaller band size pieces and collected in separate tubes. Three such replicates were
222 prepared each for GST, GST-Cpne4-vWAdomain and GST-Cpne4 pulldowns. The cut bands
223 were then processed further for liquid chromatography mass spectrometry (LC-MS). An
224 additional three replicates also prepared similarly, transferred to PVDF membranes directly after
225 SDS-PAGE and checked with specific antibodies by western blotting. See the section on western
226 blotting for further details.
227
228 **2.8 Mass spectrometry**

229 For sample preparation for LC-MS, Coomassie blue stained protein gel bands were first
230 destained with 30% ethanol solution until the gel pieces became transparent. The gel pieces were
231 then destained in 65% methanol + 10% acetic acid solution for 30 minutes. The destaining
232 solution was removed and bands were washed with 100 mM TEAB (tri-ethyl ammonium
233 bicarbonate) solution for 5 minutes. 250 ul dehydration solution (75% acetonitrile in 100 mM
234 TEAB) was added and the bands were agitated for 10 minutes at room temperature. The
235 dehydration solution was removed, and the bands were air-dryed for a couple of minutes. The gel
236 pieces were then dehydrated with reducing solution (10 mM TCEP in 100 mM TEAB) for 45
237 minutes at 56^0C. This solution was replaced by dehydration solution and bands incubated for 10
238 minutes at room temperature. The bands were then air dried and alkylation solution (20 mM
239 iodoacetamide in 100 mM TEAB) was added and incubated for 30 minutes at room temperature.
240 The gel bands were washed again and dehydrated again in the dehydration solution until the gel
241 bands shrunk to half the size. The gel bands were air dried briefly and trypsin solution was added
242 to the bands, enough to cover the bands. The bands were left on ice for 5 minutes and more
243 trypsin was added as needed. After 5 minutes, the trypsin solution was removed and 100 mM
244 TEAB was added to tubes, enough to cover the bands. The tubes were incubated at 37^0C for
245 overnight digestion. The next day, the trypsin solution was removed, and digested peptides
246 transferred to new tubes separately for each sample. 150ul of extraction solution (75%
247 acetonitrile, 0.1% formic acid) was then added to each of the tubes and agitated for 10 minutes at
248 room temperature. A short spin was done at 10,000 g and the gel pieces were saved. The extracts
249 were then vacuum dried and 25 ul 1% trifluoroacetic acid was added to each tube. This was
250 followed by a peptide clean-up as per the zip-tip protocol (Millipore Sigma; Cat# C18
251 ZTC18S008). 20ul of 0.1% formic acid (in acetonitrile) was aspirated in the zip-tip and

252 discarded. 20ul of 0.1% formic acid (in water) was similarly aspirated and discarded. The
253 peptide extract was then aspirated 7-10 times, to let the peptides bind to the zip-tip column. This
254 was followed by washing the zip-tip three times by aspiring 20ul of wash solution (0.1% formic
255 acid in water) and dispensing it. To elute the bound peptides, 20ul of elution buffer (75%
256 acetonitrile + 0.1% formic acid) was aspirated and dispensed in a tube. This step was repeated
257 five times and each time eluate was collected in the same tube. The tubes were then dried in a
258 speed vacuum. 20ul of 2% acetonitrile + 0.1% formic acid solution was added to the dried
259 peptide digest and the tubes were vortexed and centrifuged. The solution was then transferred to
260 LC vials for LC-MS analysis.

261 Desalted tryptic peptides were analyzed using nanoscale liquid chromatography tandem
262 mass spectrometry (nLC- MS/MS) and Ultimate 3000-nLC online coupled with an Orbitrap
263 Lumos Tribrid mass spectrometer (Thermo Fisher Scientific, Waltham, MA). Peptides were
264 separated on an EASY-Spray Column (Thermo Fisher Scientific; 75 μm by 50 cm inner
265 diameter, 2-μm particle size, and 100-Å pore size). Separation was achieved by 4 to 35% linear
266 gradient of acetonitrile + 0.1% formic acid for 90 minutes. An electrospray volt- age of 1.9 kV
267 was applied to the eluent via the EASY-Spray column electrode. The Orbitrap Lumos was
268 operated in positive ion data- dependent mode. Full-scan MS was performed in the Orbitrap with
269 a normal precursor mass range of 380 to 1500 *m/z* (mass/charge ratio) at a resolution of 120,000.
270 The automatic gain control (AGC) target and maximum accumulation time settings were set to 4
271 $\times 10^5$ and 50 ms, respectively. MS was triggered by selecting the most intense precursor ions
272 above an intensity threshold of 5×10^3 for collision-induced dissociation (CID)–MS
273 fragmentation with an AGC target and maximum accumulation time settings of 5×10^3 and 300
274 ms, respectively. Mass filtering was performed by the quadrupole with 1.6 m/z transmission

275 window, followed by CID fragmentation in the ion trap (rapid mode) and collision energy of
276 35%. To improve the spectral acquisition rate, parallelizable time was activated. The number of
277 MS spectra acquired between full scans was restricted to a duty cycle of 3s.

278 Raw data files were processed with the Proteome Discoverer software (v2.4, Thermo
279 Fisher Scientific), using Sequest HT (Thermo Fisher Scientific) search node for carbamylated
280 peptide/protein identifications. The following search parameters were set: protein database
281 UniProtKB/Swiss-Prot *Mus musculus* (17,033 sequences release 2020_10) concatenated with
282 reversed copies of all sequences; MS1 tolerance of 12 ppm: ion trap detected MS/MS mass
283 tolerance of 0.5Da; enzyme specificity set as trypsin with maximum two missed cleavages;
284 minimum peptide length of 6 amino acids; fixed modification of Cys (carbamidomethylation);
285 variable modification of methionine oxidation and acetyl on N terminus of protein. Percolator
286 algorithm (v.3.02.1, University of Washington) was used to calculate the false discovery rate
287 (FDR) of peptide spectrum matches (PSM), set to a q-value <0.05(2–5)

288 In order to identify retinal proteins that bind differentially to full-length Copine4 or
289 Copine4-vWA domain, we compared the peptides pulled down by either GST-vWA, GST-
290 Copine4 or GST control identified in the previous step. Of the 2119 proteins pulled down in
291 either of the three conditions, we selected for further analysis those that were represented in all
292 three replicates of at least one condition. Differential display analysis was performed using the R
293 package "DEP" (DEP 1.12.0, 10.18129/B9.bioc.DEP; (25)). Missing values were replaced with
294 0, and data was normalized using VSN normalization. Pairwise comparisons for GST only vs.
295 GST-Cpne4 and GST-vWA samples was performed at thresholds of 0.05 FDR and 2-fold
296 change.

297

298 **2.9 Western blotting**

299 Western blotting (WB) was done as described before (23). Briefly, the PVDF membranes
300 were washed with Tris buffered saline with 0.1% Tween20 (TBST). The membranes were then
301 incubated in 5% milk (in TBST) for 1 hour at room temperature. Primary antibody solution
302 prepared in 5% milk was added to the respective membranes and incubated overnight at 4C on a
303 rocker shaker. The next day, the membranes were washed three times in TBST and secondary
304 antibody solution (in 5% milk) was added. The membranes were then incubated at room
305 temperature for 1 hour, followed by three washes with TBST. The membranes were exposed to
306 Super signal chemiluminescence (Thermo Fisher Scientific) for 5 minutes and images taken on a
307 gel dock (Bio-Rad, Hercules, CA).

308

309 **2.10 Statistical analysis**

310 The statistical analysis for comparing the varicosity areas in Cpne4 with control infected
311 RGCs was done using Kolmogorov-Smirnov test (KS2, Matlab). For measuring colocalization of
312 Cpne4 to interacting proteins in co-transfected HEK293 cells, Spearmann's correlation
313 coefficient was used. Number of images, animals and cells measured and p-values are given in
314 the corresponding Results sections.

315

316

317 **3. RESULTS**

318 **3.1 Cpne4 transfection induces morphology changes *in-vitro***

319 To evaluate the subcellular distribution of Copine4 or its domains, we transfected
320 expression vectors containing full length Cpne4, C2 domains or vWA domain tagged with HA

321 (Fig.1A, B), in conjunction with a plasma membrane attached eGFP variant (meGFP) into
322 HEK293 cells. Full length Copine4, C2 domains or vWA domain were detected in the nuclei,
323 cell body as well as plasma membrane of the cells (Fig.1C) as indicated by both HA (red) and
324 Cpne4 (white) staining. As previously reported, full length Cpne4 induces morphological
325 changes (Fig. 1C top panel; n=2 experiments) resembling neurites (23). C2 domain or vWA
326 domain constructs also induce extended process formation occasionally, although morphological
327 changes were not as prominent and wide spread as with Cpne4 transfection (Fig.1C middle and
328 bottom panel; n=2 experiments each).
329
330 **3.2 Cpne4 infection induces morphology changes *in-vivo* in RGCs**
331 Given the morphological defects observed when expressing Copines in HEK293 cells in
332 culture, we asked whether overexpressing Cpne4 in RGCs will affect RGC morphology. We
333 therefore infected either P0 or P14 Brn3b$^{Cre/WT}$ mice with AAV1 vectors co-expressing HA-
334 tagged Cpne4 and meGFP in a Cre-dependent manner. Membranes from infected Brn3b$^{Cre/WT}$
335 RGCs were labelled with eGFP (green), revealing axonal arbors, cell bodies and dendrites
336 (Fig.2A, B). In contrast, Cpne4 expression as seen by HA (red) labeling was largely confined to
337 the cell body and dendrites, and only rarely reached into the axon (Fig.2A, B; n=6 retinas, 72
338 cells). Interestingly, several large varicosities were observed on dendrites of Cpne4 infected
339 Brn3b$^{Cre/WT}$ RGCs. These large varicosities (we call these 'blebs', Fig. 2A, 2A1) can be easily
340 distinguished from regular varicosities, as seen on the RGC dendrites in Cpne4 infected cells
341 (Fig. 2A, 2A2, supplementary Figure 1A, n=6 animals, 72 cells), or on the dendrites of control
342 RGCs infected solely with AAV1-eGFP (Fig.2C, E; area= 10.7± 0.61um^2 for Cpne4 versus
343 3.12± 0.18um^2 for controls, KS2 test p value < 0.05; controls n=8 animals, 73 cells). The size

344 and number of blebs varied significantly across the infected RGCs, and bleb size tended to
345 increase with RGC dendritic arbor area (Supplementary Figure 1B, C). A comparison between
346 the P0 and P15 Cpne4 infected RGCs suggest no differences in the bleb areas (P0 mean area=
347 9.95± 1.11um^2, P15 mean bleb area= 15± 3.75um^2; p=0.2), suggesting that the process disrupted
348 by Cpne4 overexpression is still active in nearly adult animals (P14), as opposed to the early
349 stages of dendrite formation (P0). A high resolution (Zeiss LSM 880 airy scan) imaging
350 revealed that blebs contained large amounts of Cpne4, as well as cell membranes, as revealed by
351 membrane attached eGFP. Besides the formation of large varicosities or blebs, Cpne4 over-
352 expression into RGCs did not cause any changes in the arbor area or stratification when
353 compared to controls infected with eGFP (Fig.2F, G). Infection of RGCs with AAV1 vectors
354 expressing either C2 domains or vWA domains alone did not cause significant morphological
355 changes or formation of bigger blebs (data not shown).
356

357 **3.3 Yeast two hybrid analysis reveals Cpne4 vWA domain interaction with Morn2, HCFC1**
358 **and Tox3**

359 The domain structure of Copines, and previous work on other family members suggests
360 that Copine C2 domains facilitate Ca^{2+} mediated membrane attachment, while Copine vWA
361 mediates interactions with other proteins. We therefore used a Gal4 based yeast two hybrid
362 system using the Cpne4 vWA domain as bait protein and an adult mouse retina cDNA library as
363 pray, in order to identify potential retina-specific interactors of Cpne4. Only five clones selected
364 from the initial screening confirmed upon replating (Fig.3A). A colony PCR (Fig.3B) and
365 subsequent Sanger sequencing on the PCR products identified the clones as domains of five
366 proteins- 2 clones of HCFC1, 1 each of Morn2, Tox3 and GAPDH and a mixed clone consisting

367 of Rhodopsin and GAPDH (Fig.3B). Interestingly, the interacting domain of Tox3 protein
368 contained the HMG box and that for HCFC1 contained an HCF repeat4. For Morn2 the
369 interacting domain consisted of full length of the Morn2 protein and some non-coding sequence
370 on the 5' end (Fig.3C). Complete cDNA sequences of the regions of Morn2, HCFC1 and Tox3
371 interacting with Cpne4 are given in the Supplementary document.
372
373 **3.4 Cpne4 vWA domain interacts with HCFC1, Morn2 and Mycbp2 in HEK293 cells**
374 We next sought to validate our candidate Cpne4 interactors (HCFC1, Morn2 and Tox3)
375 by co-immunoprecipitation. In addition, we surveyed candidate Cpne4-vWA interactors
376 identified in a previous yeast two hybrid analysis using a mouse embryonic cDNA library (26).
377 By exploring our RNA sequencing analysis (1), we found that some of these previously reported
378 candidate Cpne4 interactors (Bicd2, Pitpnm2, Sptbn1 and Mycbp2) were indeed expressed in
379 RGCs (Supp. Fig. 2, Fig. 5A). We therefore cloned the interacting peptide regions from our
380 candidates (HCFC1, Morn2 and Tox3) as well as the matches from the Tomsig et al. study
381 (Bicd2, Pitpnm2, Sptbn1 and Mycbp2) downstream of the Flag tag in an eukaryotic expression
382 vector and co-transfected them with the HA-tagged Cpne4-vWA in HEK293 cells.
383 The colocalization of these proteins was observed by immunostaining (Fig.4B, C, and E;
384 n=6, 5 and 4 for Morn2, HCFC1 and Tox3 respectively). While Mycbp2 and Morn2 were
385 localized in the cell body of the cells, Tox3 was always localized in the nuclei (Fig.4E; n=6).
386 Colocalization analysis between Cpne4 and potential interactors showed that both
387 HCFC1 and Morn2 had some degree of colocalization with Cpne4 (mean Spearmann's
388 correlation coefficient R= 0.19 for HCFC1, n=15 ROIs; mean R= 0.32 for Morn2, n=25 ROIs)
389 whereas Tox3 did not (mean R= -0.19, n=26 images; Fig.4F, G). Furthermore, a pull-down

390 analysis with Flag antibody showed that the identified Morn2 and HCFC1 domains can interact
391 with the Cpne4 vWA domain while Tox3 does not (Fig.4H, I, J; n=4 for Morn2, n=3 for Tox3).
392 Of the four Tomsig candidates, only Mycbp2 exhibited a small degree of colocalization with
393 Cpne4 (mean R= 0.07, n=13 images; Fig.4D). Mycbp2 was also pulled down with Cpne4 vWA
394 domain (Fig. 4H, I; n=4). The other candidates - Bicd2, Pitpnm2 and Sptbn1 - were not pulled
395 down with Cpne4 vWA domain (data not shown).

396 RNA expression as observed by RNA sequencing analysis (Fig.5A) (1) reveals that
397 HCFC1, Morn2 and Mycbp2 are expressed in RGCs as well as the rest of the retina at E15 and at
398 P3 (Fig.5A). Immunostaining for HCFC1 (red) in the retina showed that it was localized in the
399 Brn3b^{+} RGCs (green) in the ganglion cell layer in both Brn3b WT as well as Brn3b KO retinas
400 (Fig.5B; n=2). Immunostaining for Morn2 (green) showed expression in the IPL and GCL in
401 both Brn3b$^{WT/WT}$ and Brn3b$^{KO/KO}$ retinas (Fig.5C; n=2).

402

403 **3.5 Mass Spectrometry analysis of retinal proteins identifies potential Cpne4 interactions.**

404 Copine4 protein interactions with the vWA domain may be modulated by the C2
405 domains. In order to identify potential native, full length Copine4 protein binding partners in the
406 retina, we performed pulldown assays of mouse retina protein extracts with GST-vWA or GST-
407 Cpne4 fusion proteins, alongside GST-only controls using Glutathione-Sepharose beads
408 (Fig.6A). Each experimental condition was repeated in triplicate, and Glutathione eluates were
409 loaded onto polyacrylamide gels, separated by electrophoresis, gel bands cut out and processed
410 for LC-MS. A total of 2119 proteins were represented in the LC-MS results by at least one
411 peptide (Supplementary table 1). In order to increase the stringency of our screen, we considered
412 for analysis only proteins that were represented by at least one peptide in all three replicates of at

413 least one of the pull-down conditions (GST-Cpne4, GST-vWA or GST only; 278 total).
414 Differential expression was performed using the Bioconductor R package DEP (see material and
415 methods), and a fold change of 2 and FDR of 5 % were used as thresholds for differential
416 expression. Based on these criteria, 27 proteins were enriched in both GST-Cpne4 and GST-
417 vWA relative to GST controls, while 180 proteins were significantly enriched in GST-Cpne4 but
418 not GST-vWA samples relative to GST controls (Fig.6A, C, D, Supp. Table 1; n= 3 experiments,
419 19 retinas per experiment).

420 GO analysis performed on the 207 proteins that interacted with Cpne4 or Cpne4-vWA
421 (Supp. Table 2) identified 412 biological processes and 146 molecular functions significantly
422 enriched (FDR $p<0.05$). Amongst the top 30 most significantly enriched biological processes
423 (FDR <= 5.21 e-09) all but two were related to metabolic processes, including glycolysis, ATP
424 or nucleotide metabolism. The two biological processes unrelated to metabolism but interesting
425 from the perspective of Cpne4 involvement in cell morphology and differentiation were
426 "regulation of localization" (FDR <= 2.32 e-11) and "regulation of transport" (FDR <= 4.29 e-
427 10). Molecular functions were mostly associated with nucleotide binding, protein binding,
428 enzymatic or catalytic activity. Of the 180 GO cellular components that appeared enriched
429 amongst Cpne4 interactors, at the very top were compartments associated with myelin sheath,
430 cytoplasm, synapse, plasma membrane bounded cell projection, and neuron projection (FDRs <=
431 2.84 e-19). Interestingly, the highest fold enrichment and low FDR for Cpne4 and its interactors
432 also suggested its localization in the late endosome lumen. A GO pathways analysis (PANTHER
433 GO pathways) reveals that potential Cpne4 interactions participate overwhelmingly in a variety
434 of neuronal seven transmembrane receptor pathways (Muscarinic, Metabotropic Glutamate
435 Receptor, Opioid, Serotonine and Dopamine, etc.) at FDRs <= 8.03 e-05. PI3 Kinase and

436 cytoskeletal regulation by Rho GTPase pathways were also significantly enriched. The complete
437 list of all these suggested functions and locations from GO analysis are listed in Supplementary
438 table 2.

439 In order to validate our MS screen, we analyzed several proteins associated with some of
440 the enriched processes: 14-3-3 family of proteins, Map1b, SV2 and Syntaxin-1 (Supp fig. 3).
441 Their association with either GST-vWA or GST-Cpne4 in the retina was confirmed by Western
442 blotting of pulldowns from retinal lysates (Fig.6B). RNA sequencing data showed that the RNA
443 for these candidates was enriched in the retina (Supp. Fig. 2). Using immunohistochemistry, pan
444 14-3-3 and Map1b (red) were found to colocalize in the Cpne4^{+} RGCs (green; Fig.7A, B; n=3
445 retinas each) in Brn3b WT and KO retina. SV2 and Syntaxin (red) were colocalized in the IPL of
446 both Brn3b WT and KO (Fig. 7C, D; n=3 retinas each).

447

448

449 **4. DISCUSSION**

450 Amongst Copine family members, Cpne4 has one of the highest mRNA expressions in
451 the retina and is predominantly expressed in the RGC layer (23). Cpne4 over-expression in
452 RGCs lead to formation of large varicosities on dendrites but no other morphological changes to
453 RGC dendritic arbor area or stratification. The morphological defects observed by
454 overexpression in HEK293 cells require a full length Cpne4 protein, as neither C2 domains nor
455 vWA domain can induce extensive process formation in isolation. Cpne4 may be involved in
456 several distinct metabolic and signaling pathways, as revealed by our Yeast two-hybrid and
457 retina proteome interaction studies. Several proteins can interact directly with Cpne4 including
458 Morn2, HCFC1, 14-3-3 family, Map1b, Syntaxin1 and SV2.

459

460 **4.1 Cpne4 regulates cytoskeletal structure in the cells**

461 It is known that Brn3 transcription factors cause morphological changes in the retina
462 during development and these changes are most likely achieved through their transcriptional
463 targets (2,23,27,28). Cpne4 is one such molecule that is regulated by both Brn3a and Brn3b (1).
464 Results from the current study and previously reported experiments show that over-expression of
465 various Copines in vitro in HEK293 cells leads to elongation of the transfected cells and
466 formation of neurite like structures (23). Transfection with the dominant negative forms of
467 Cpne4 however, did not result in substantial morphology changes. This suggests that the
468 association of C2 domains and vWA domain are critical for inducing phenotypic changes in
469 vitro. Interestingly, the GO analysis of Cpne4 and its interacting proteins suggests its localization
470 in plasma membrane bounded cell projection, and neuron projection, among other locations
471 indicating that it might be involved in cytoskeleton – plasma membrane interactions within the
472 cells.

473 Large varicosities, similar to the ones observed on RGC dendrites following Cpne4 over-
474 expression, are reminiscent of previously described dendrite swellings, under normal and
475 pathogenetic conditions. In Drosophila larvae, dendrite arborizations of superficial sensory
476 neurons are heavily remodeled during metamorphosis. Prior to pruning, the dendrites tagged for
477 elimination experience marked calcium transients, followed by increased endocytosis and
478 formation of varicosities, like beads on a string. The beaded dendrites are eventually resorbed
479 prior to formation of the new arbor (29,30). Similar large varicosities are also observed on the
480 dendrites of neurons undergoing NMDA-induced excitotoxicity (31,32).

481 Other Copines have been previously shown to be involved in morphological changes.
482 Cpne6 mediates cytoskeletal changes in the hippocampus during LTP (18,19). Cpne6 interacts
483 with Rac1 to regulate the Rac1/LimK/Cofilin signaling pathway that further regulates
484 microtubule polymerization and hence affects the spine formation in hippocampal neurons (18).
485 Cpne3 along with Rac1 is required for cell migration during tumor metastasis (33). Copine A, a
486 Copine homolog in Dictyostelium, interacts with actin filaments and regulates chemotaxis and
487 adhesion in these organisms (16). CPNA1, Copine homolog in C. elegans, is located at integrin
488 adhesion sites in the muscle cells and acts as a linker between various myofilament proteins to
489 maintain muscle stability (14).
490 Taken together, these studies suggest that Copines may mediate membrane – cytoskeletal
491 interactions in a variety of contexts. It is not clear whether the large varicosities on RGCs
492 indicate a role of Cpne4 in dendrite remodeling, or cytoskeletal changes during dendrite
493 development of the retina. Expression of Cpne4 and several other Copine family members
494 increases dramatically during the first two postnatal weeks, a period of intense RGC dendritic
495 arbor growth, differentiation and maturation of dendritic arbor at the time of eye opening.
496 However, the varicosities appeared irrespective of whether the Cpne4 was over-expressed at P0
497 when the eyes are closed and the inner retina is still developing or at P14 when the eyes are open
498 and pruning of the dendrites happens.
499
500 **4.2 Cpne4 and endosomal/lysosomal/autophagosomal pathways**
501 Yeast two hybrid analysis on a retina cDNA library indicated Cpne4 interacts with
502 Morn2. Morn2 RNA is expressed in the RGCs and protein expression is seen in the RGCs and
503 dendritic arbor in the IPL. Morn2 consists of a single conserved domain- a MORN (Membrane

504 Occupation and Recognition Nexus) motif. Morn2 interacts with LC3 to recruit phagosomes
505 against various bacteria in planarian flatworms (34), and is involved in cell membrane
506 engulfment of bacteria and eventually in the invasion of bacteria into the cells (35). Other Morn
507 repeat containing proteins with known functions are junctophilin, retinophilin (also known as
508 Morn4 or Undertaker), PIPK (phosphatidylinositol monophosphate kinase), and Alsin2.

509 We and a previous study (26) have confirmed that Mycbp2 interacts with Cpne4. Mycbp2
510 is a Ubiquitin ligase that contains several conserved domains that are required for a variety of
511 functions (36). Rpm-1, the C. elegans homolog of Mycbp2, regulates AMPA receptor trafficking
512 by regulating the degradation of DLK1 which further regulates Rab5 endosomal protein (37,38).
513 Rab5 endosomes are required for dendritic branching (39).

514 Copine A, in Dictyostelium also associates with vacuoles, endolysosomal organelles and
515 phagosomes in Ca^{2+} dependent way (40). Cpne6 translocates to clathrin coated vesicles when
516 Ca^{2+} concentration increases in the cells (6). Previous reports suggest Cpne1 involvement in
517 endosomal and autophagocytosis pathways. Specifically, Cpne1 together with AnnexinA1 and
518 AnnexinA5 and is involved in calcium dependent autophagosomal degradation (41,42). Cpne1 is
519 also involved in endoproteolysis of NFκB (43).

520 Further studies need to be done to see if Cpne4 is involved in similar function in the
521 retina. One of the top hits for probable sub-cellular location of Cpne4 based on the GO analysis
522 of its interacting proteins is the late endosome lumen. Another possible function of Cpne4 as
523 indicated by GO analysis suggests its role in regulation of transport in the neurons. In this
524 context, the dendritic varicosities induced in RGCs could be the result of disrupted vesicle
525 trafficking. We note that super-resolution imaging of varicosities reveal accumulation of
526 membranes, besides Cpne4 itself.

527

528 **4.3 Cpne4 and neuronal maturation and synapse formation**

529 Copines were initially discovered in the cell bodies and dendrites of hippocampus
530 neurons and dendrites (10,17) and have been implicated in a variety of functions in the brain.
531 Cpne6 may be involved in long term potentiation (18,19) and suppression of spontaneous
532 neurotransmitter release (44). Cpne1 is upregulated during neural tube closure in mouse
533 embryo, regulates neural stem cell functions during development and it is also required for
534 progenitor cell differentiation of neurons in the hippocampus (20,21,45). The role of Copines in
535 the development or physiology of retina is unknown. But the interactions of Cpne4 with various
536 proteins indicate several possible functions in the retina.

537 Several protein interactions with Cpne4 were observed with LC-MS analysis. Some of
538 these that were particularly interesting and were expressed in the retina specifically in the inner
539 retina were the 14-3-3 family, Map1b, Syntaxin1 and SV2. 14-3-3 family of proteins is one of
540 the most abundant proteins in the central nervous system. 14-3-3Ɛ, that was found to interact
541 with Cpne4, is previously known to bind to doublecortin (Dcx) protein, prevents its degradation
542 which further prevents neurite formation by preventing the microtubules from invading the
543 lamellipodia (46). 14-3-3Ɛ and 14-3-3ζ are known to regulate neurogenesis and differentiation of
544 neuronal progenitor cells in the cortex. This is achieved by regulating the catenin/Rho
545 GTPase/Limk1/cofilin signaling pathway to promote F-actin formation (47). 14-3-3ɣ regulates
546 Cpne1 to enhance differentiation of hippocampal progenitor cells and neurite formation in these
547 cells (21,48). Map1b plays an important role in axon guidance and axonal branching during the
548 development of the nervous system (49,50). Synaptic proteins Syntaxin1 and SV2, also
549 interacting with Cpne4, are required in neurotransmitter release at the presynaptic terminal in the

550 retina (51,52). Interestingly, according to GO analysis of Cpne4 and its interacting proteins, one
551 of the highest probability of localization of Cpne4 is at the synapse. This also correlates with the
552 previous reports on localization and interaction of Cpne6 with various SNARE proteins on the
553 presynaptic membrane as well as PSD in the postsynaptic membrane (18,44).

554 The yeast two hybrid analysis revealed HCFC1 as an interaction of Cpne4. HCFC1 RNA
555 and protein is also expressed in retina and RGCs. HCFC1 was initially discovered as
556 transcriptional co-activator that along with Oct1 forms a complex with VP16 from Herpes
557 simplex virus and help utilize the transcriptional machinery of the host cell for replicating the
558 virus (53). In neurons, over-expression of HCFC1 leads to neuronal maturation and also limits
559 neurite growth (54). Mutations in HCFC1 protein are associated with Non syndromic Intellectual
560 Disability in humans (55).

561 The functions of Mycbp2 in the central nervous system have been studied extensively
562 before (36). In retina, Mycbp2 RNA expression is observed in RGCs and other cell types and is
563 required for axonal growth cone formation (56). Knocking out Mycbp2 prevents RGC axons
564 from reaching the thalamus and mis-targeted axons in mouse LGN (57–59). Highwire, the
565 homolog of Mycbp2 in Drosophila is also required for synapse formation (60,61).

566

567

568 **5. CONCLUSIONS**

569 To summarize, Cpne4 over-expression leads to morphological changes in the retina.
570 Cpne4 interacts with multiple proteins and is involved in several different pathways within the
571 cells. This study points to several interesting directions, in relation to possible function of Cpne4

572 in the retina and the rest of the nervous system. Each specific interaction needs to be explored
573 further to establish their roles in development and functioning of the retina.
574

575 **ACKNOWLEDGEMENTS**

576 This study was funded by NIH intramural funding support to Tudor C. Badea (EY000504). We
577 want to thank Nadia Parmhans for assistance with genotyping, Jacob Nellissery for sharing the
578 co-immunoprecepitation protocols and Quira Zeidan (NICHD, NIH) for providing the yeast
579 strains AH109 and Y187 and her valuable inputs on growing and mating yeast cells.
580

581 **REFERENCES**

582 1. Sajgo S, Ghinia MG, Brooks M, Kretschmer F, Chuang K, Hiriyanna S, Wu Z, Popescu
583 O, Badea TC. Molecular codes for cell type specification in Brn3 retinal ganglion cells.
584 Proc Natl Acad Sci U S A. 2017;114(20):E3974–83.
585 2. Muzyka VV, Brooks M, Badea TC. Postnatal developmental dynamics of cell type
586 specification genes in Brn3a/Pou4f1 Retinal Ganglion Cells. Neural Dev. 2018;13(1):1–
587 33.
588 3. Liu J, Reggiani JDS, Laboulaye MA, Pandey S, Chen B, Rubenstein JLR, Krishnaswamy
589 A, Sanes JR. Tbr1 instructs laminar patterning of retinal ganglion cell dendrites. Nat
590 Neurosci. 2018 May;21(5):659–70.
591 4. Creutz CE, Tomsig JL, Snyder SL, Gautier MC, Skouri F, Beisson J, Cohen J. The
592 copines, a novel class of C2 domain-containing, calcium-dependent, phospholipid-binding
593 proteins conserved from Paramecium to humans. J Biol Chem. 1998;273(3):1393–402.
594 5. Tomsig JL, Creutz CE. Copines: A ubiquitous family of Ca2+-dependent phospholipid-

595 binding proteins. Cell Mol Life Sci. 2002;59(9):1467–77.
596 6. Perestenko P, Watanabe M, Beusnard-Bee T, Guna P, McIlhinney J. The second C2-
597 domain of copine-2, copine-6 and copine-7 is responsible for their calcium-dependent
598 membrane association. FEBS J. 2015;282(19):3722–36.
599 7. Whittaker CA, Hynes RO. Distribution and evolution of von Willebrand/integrin A
600 domains: widely dispersed domains with roles in cell adhesion and elsewhere. Mol Biol
601 Cell. 2002 Oct;13(10):3369–87.
602 8. Maitra R, Grigoryev DN, Bera TK, Pastan IH, Lee B. Cloning, molecular characterization,
603 and expression analysis of Copine 8. Biochem Biophys Res Commun. 2003;303(3):842–7.
604 9. Savino M, D'Apolito M, Centra M, Van Beerendonk HM, Cleton-Jansen AM, Whitmore
605 SA, Crawford J, Callen DF, Zelante L, Savoia A. Characterization of copine VII, a new
606 member of the copine family, and its exclusion as a candidate in sporadic breast cancers
607 with loss of heterozygosity at 16q24.3. Genomics. 1999;61(2):219–26.
608 10. Nakayama T, Yaoi T, Yasui M, Kuwajima G. N-copine: a novel two C2-domain-
609 containing protein with neuronal activity-regulated expression. FEBS Lett. 1998
610 May;428(1–2):80–4.
611 11. Cowland JB, Carter D, Bjerregaard MD, Johnsen AH, Borregaard N, Lollike K. Tissue
612 expression of copines and isolation of copines I and III from the cytosol of human
613 neutrophils Abstract : Copines are a recently identified group of proteins characterized by
614 two Ca 2 -binding C2- C terminus . Although pEST sequences indicate the. J Leukoc Biol.
615 2003;74(September):379–88.
616 12. Zhang Y, Chen K, Sloan SA, Bennett ML, Scholze AR, O'Keeffe S, Phatnani HP,
617 Guarnieri P, Caneda C, Ruderisch N, Deng S, Liddelow SA, Zhang C, Daneman R,

618 Maniatis T, Barres BA, Wu JQ. An RNA-sequencing transcriptome and splicing database
619 of glia, neurons, and vascular cells of the cerebral cortex. J Neurosci. 2014
620 Sep;34(36):11929–47.
621 13. Hua J, Grisafi P, Cheng SH, Fink GR. Plant growth homeostasis is controlled by the
622 arabidopsis BON1 and BAP1 genes. Genes Dev. 2001;15(17):2263–72.
623 14. Warner A, Xiong G, Qadota H, Rogalski T, Vogl AW, Moerman DG, Benian GM.
624 CPNA-1, a copine domain protein, is located at integrin adhesion sites and is required for
625 myofilament stability in Caenorhabditis elegans. Mol Biol Cell. 2013;24(5):601–16.
626 15. Ilacqua AN, Price JE, Graham BN, Buccilli MJ, McKellar DR, Damer CK. Cyclic AMP
627 signaling in Dictyostelium promotes the translocation of the copine family of calcium-
628 binding proteins to the plasma membrane. BMC Cell Biol. 2018;19(1):1–16.
629 16. Buccilli MJ, Ilacqua AN, Han M, Banas AA, Wight EM, Mao H, Perry SP, Salter TS,
630 Loiselle DR, Haystead TAJ, Damer CK. Copine A Interacts with Actin Filaments and
631 Plays a Role in Chemotaxis and Adhesion. Cells. 2019;8(7):758.
632 17. Nakayama T, Yaoi T, Kuwajima G, Yoshie O, Sakata T. Ca2+-dependent interaction of
633 N-copine, a member of the two C2 domain protein family, with OS-9, the product of a
634 gene frequently amplified in osteosarcoma. FEBS Lett. 1999;453(1–2):77–80.
635 18. Reinhard JR, Kriz A, Galic M, Angliker N, Rajalu M, Vogt KE, Ruegg MA. The calcium
636 sensor Copine-6 regulates spine structural plasticity and learning and memory. Nat
637 Commun. 2016 May;7:11613.
638 19. Burk K, Ramachandran B, Ahmed S, Hurtado-Zavala JI, Awasthi A, Benito E, Faram R,
639 Ahmad H, Swaminathan A, McIlhinney J, Fischer A, Perestenko P, Dean C. Regulation of
640 Dendritic Spine Morphology in Hippocampal Neurons by Copine-6. Cereb Cortex. 2018

641 Apr;28(4):1087–104.
642 20. Greene NDE, Leung K-Y, Wait R, Begum S, Dunn MJ, Copp AJ. Differential protein
643 expression at the stage of neural tube closure in the mouse embryo. J Biol Chem. 2002
644 Nov;277(44):41645–51.
645 21. Park N, Yoo JC, Ryu J, Hong S-G, Hwang EM, Park J-Y. Copine1 enhances neuronal
646 differentiation of the hippocampal progenitor HiB5 cells. Mol Cells. 2012 Dec;34(6):549–
647 54.
648 22. Liu C-Y, Tsai C-J, Yasugaki S, Nagata N, Morita M, Isotani A, Yanagisawa M, Hayashi
649 Y. Copine-7 is required for REM sleep regulation following cage change or water
650 immersion and restraint stress in mice. Neurosci Res. 2021 Apr;165:14–25.
651 23. Goel M, Li T, Badea TC. Differential expression and subcellular localization of Copines
652 in mouse retina. J Comp Neurol. 2019;527(14):2245–62.
653 24. Gan L, Xiang M, Zhou L, Wagner DS, Klein WH, Nathans J. POU domain factor Brn-3b
654 is required for the development of a large set of retinal ganglion cells. Proc Natl Acad Sci
655 U S A. 1996 Apr;93(9):3920–5.
656 25. Zhang X, Smits AH, van Tilburg GB, Ovaa H, Huber W, Vermeulen M. Proteome-wide
657 identification of ubiquitin interactions using UbIA-MS. Nat Protoc. 2018 Mar;13(3):530–
658 50.
659 26. Tomsig JL, Snyder SL, Creutz CE. Identification of targets for calcium signaling through
660 the copine family of proteins. Characterization of a coiled-coil copine-binding motif. J
661 Biol Chem. 2003;278(12):10048–54.
662 27. Badea TC, Cahill H, Ecker J, Hattar S, Nathans J. Distinct Roles of Transcription Factors
663 Brn3a and Brn3b in Controlling the Development, Morphology, and Function of Retinal

664 Ganglion Cells. Neuron [Internet]. 2009;61(6):852–64. Available from:
665 http://dx.doi.org/10.1016/j.neuron.2009.01.020
666 28. Badea TC, Nathans J. Morphologies of mouse retinal ganglion cells expressing
667 transcription factors Brn3a, Brn3b, and Brn3c: analysis of wild type and mutant cells
668 using genetically-directed sparse labeling. Vision Res. 2011 Jan;51(2):269–79.
669 29. Kanamori T, Yoshino J, Yasunaga KI, Dairyo Y, Emoto K. Local endocytosis triggers
670 dendritic thinning and pruning in Drosophila sensory neurons. Nat Commun [Internet].
671 2015;6(May 2014):1–14. Available from: http://dx.doi.org/10.1038/ncomms7515
672 30. Williams DW, Truman JW. Remodeling dendrites during insect metamorphosis. J
673 Neurobiol. 2005 Jul;64(1):24–33.
674 31. Olney JW, Fuller T, de Gubareff T. Acute dendrotoxic changes in the hippocampus of
675 kainate treated rats. Brain Res. 1979 Oct;176(1):91–100.
676 32. Ahlgren H, Bas-Orth C, Freitag HE, Hellwig A, Ottersen OP, Bading H. The nuclear
677 calcium signaling target, activating transcription factor 3 (ATF3), protects against
678 dendrotoxicity and facilitates the recovery of synaptic transmission after an excitotoxic
679 insult. J Biol Chem. 2014;289(14):9970–82.
680 33. Ahmat Amin MKB, Shimizu A, Zankov DP, Sato A, Kurita S, Ito M, Maeda T, Yoshida
681 T, Sakaue T, Higashiyama S, Kawauchi A, Ogita H. Epithelial membrane protein 1
682 promotes tumor metastasis by enhancing cell migration via copine-III and Rac1.
683 Oncogene. 2018;37(40):5416–34.
684 34. Abnave P, Mottola G, Gimenez G, Boucherit N, Trouplin V, Torre C, Conti F, Ben Amara
685 A, Lepolard C, Djian B, Hamaoui D, Mettouchi A, Kumar A, Pagnotta S, Bonatti S,
686 Lepidi H, Salvetti A, Abi-Rached L, Lemichez E, Mege JL, Ghigo E. Screening in

687 planarians identifies MORN2 as a key component in LC3-associated phagocytosis and
688 resistance to bacterial infection. Cell Host Microbe [Internet]. 2014;16(3):338–50.
689 Available from: http://dx.doi.org/10.1016/j.chom.2014.08.002
690 35. McGuire AM, Cochrane K, Griggs AD, Haas BJ, Abeel T, Zeng Q, Nice JB, Macdonald
691 H, Birren BW, Berger BW, Allen-Vercoe E, Earl AM. Evolution of invasion in a diverse
692 set of Fusobacterium species. MBio. 2014;5(6):1–11.
693 36. Po MD, Hwang C, Zhen M. PHRs: bridging axon guidance, outgrowth and synapse
694 development. Curr Opin Neurobiol. 2010;20(1):100–7.
695 37. Grill B, Bienvenut W V., Brown HM, Ackley BD, Quadroni M, Jin Y. C. elegans RPM-1
696 Regulates Axon Termination and Synaptogenesis through the Rab GEF GLO-4 and the
697 Rab GTPase GLO-1. Neuron. 2007;55(4):587–601.
698 38. Park EC, Glodowski DR, Rongo C. The ubiquitin ligase RPM-1 and the p38 MAPK
699 PMK-3 regulate AMPA receptor trafficking. PLoS One. 2009;4(1).
700 39. Satoh D, Sato D, Tsuyama T, Saito M, Ohkura H, Rolls MM, Ishikawa F, Uemura T.
701 Spatial control of branching within dendritic arbors by dynein-dependent transport of
702 Rab5-endosomes. Nat Cell Biol. 2008 Oct;10(10):1164–71.
703 40. Damer CK, Bayeva M, Hahn ES, Rivera J, Socec CI. Copine A, a calcium-dependent
704 membrane-binding protein, transiently localizes to the plasma membrane and intracellular
705 vacuoles in Dictyostelium. BMC Cell Biol. 2005;6:1–18.
706 41. Creutz CE, Edwardson JM. Organization and synergistic binding of copine I and annexin
707 A1 on supported lipid bilayers observed by atomic force microscopy. Biochim Biophys
708 Acta - Biomembr [Internet]. 2009;1788(9):1950–61. Available from:
709 http://dx.doi.org/10.1016/j.bbamem.2009.06.009

710 42. Ghislat G, Knecht E. New Ca2+-dependent regulators of autophagosome maturation.
711 Commun Integr Biol. 2012;5(4):308–11.
712 43. Ramsey CS, Yeung F, Stoddard PB, Li D, Creutz CE, Mayo MW. Copine-I represses NF-
713 κB transcription by endoproteolysis of p65. Oncogene. 2008;27(25):3516–26.
714 44. Liu P, Khvotchev M, Li YC, Chanaday NL, Kavalali ET. Copine-6 Binds to SNAREs and
715 Selectively Suppresses Spontaneous Neurotransmission. J Neurosci. 2018
716 Jun;38(26):5888–99.
717 45. Kim TH, Sung S-E, Cheal Yoo J, Park J-Y, Yi G-S, Heo JY, Lee J-R, Kim N-S, Lee DY.
718 Copine1 regulates neural stem cell functions during brain development. Biochem Biophys
719 Res Commun. 2018 Jan;495(1):168–73.
720 46. Cornell B, Wachi T, Zhukarev V, Toyo-Oka K. Regulation of neuronal morphogenesis by
721 14-3-3epsilon (Ywhae) via the microtubule binding protein, doublecortin. Hum Mol
722 Genet. 2016 Oct;25(20):4405–18.
723 47. Toyo-oka K, Wachi T, Hunt RF, Baraban SC, Taya S, Ramshaw H, Kaibuchi K, Schwarz
724 QP, Lopez AF, Wynshaw-Boris A. 14-3-3ε and ζ regulate neurogenesis and differentiation
725 of neuronal progenitor cells in the developing brain. J Neurosci. 2014 Sep;34(36):12168–
726 81.
727 48. Cheal Yoo J, Park N, Lee B, Nashed A, Lee Y-S, Hwan Kim T, Yong Lee D, Kim A, Mi
728 Hwang E, Yi G-S, Park J-Y. 14-3-3γ regulates Copine1-mediated neuronal differentiation
729 in HiB5 hippocampal progenitor cells. Exp Cell Res. 2017 Jul;356(1):85–92.
730 49. Meixner A, Haverkamp S, Wässle H, Führer S, Thalhammer J, Kropf N, Bittner RE,
731 Lassmann H, Wiche G, Propst F. MAP1B is required for axon guidance and Is involved in
732 the development of the central and peripheral nervous system. J Cell Biol. 2000

733 Dec;151(6):1169–78.
734 50. Bouquet C, Soares S, von Boxberg Y, Ravaille-Veron M, Propst F, Nothias F.
735 Microtubule-associated protein 1B controls directionality of growth cone migration and
736 axonal branching in regeneration of adult dorsal root ganglia neurons. J Neurosci. 2004
737 Aug;24(32):7204–13.
738 51. Sherry DM, Mitchell R, Standifer KM, du Plessis B. Distribution of plasma membrane-
739 associated syntaxins 1 through 4 indicates distinct trafficking functions in the synaptic
740 layers of the mouse retina. BMC Neurosci. 2006 Jul;7:54.
741 52. Wang MM, Janz R, Belizaire R, Frishman LJ, Sherry DM. Differential distribution and
742 developmental expression of synaptic vesicle protein 2 isoforms in the mouse retina. J
743 Comp Neurol. 2003 May;460(1):106–22.
744 53. Wysocka J, Herr W. The herpes simplex virus VP16-induced complex: The makings of a
745 regulatory switch. Trends Biochem Sci. 2003;28(6):294–304.
746 54. Huang L, Jolly LA, Willis-Owen S, Gardner A, Kumar R, Douglas E, Shoubridge C,
747 Wieczorek D, Tzschach A, Cohen M, Hackett A, Field M, Froyen G, Hu H, Haas SA,
748 Ropers HH, Kalscheuer VM, Corbett MA, Gecz J. A noncoding, regulatory mutation
749 implicates HCFC1 in nonsyndromic intellectual disability. Am J Hum Genet [Internet].
750 2012;91(4):694–702. Available from: http://dx.doi.org/10.1016/j.ajhg.2012.08.011
751 55. Yu HC, Sloan JL, Scharer G, Brebner A, Quintana AM, Achilly NP, Manoli I, Coughlin
752 CR, Geiger EA, Schneck U, Watkins D, Suormala T, Van Hove JLK, Fowler B,
753 Baumgartner MR, Rosenblatt DS, Venditti CP, Shaikh TH. An X-linked cobalamin
754 disorder caused by mutations in transcriptional coregulator HCFC1. Am J Hum Genet
755 [Internet]. 2013;93(3):506–14. Available from:

756 http://dx.doi.org/10.1016/j.ajhg.2013.07.022
757 56. Lewcock JW, Genoud N, Lettieri K, Pfaff SL. The Ubiquitin Ligase Phr1 Regulates Axon
758 Outgrowth through Modulation of Microtubule Dynamics. Neuron. 2007;56(4):604–20.
759 57. Bloom AJ, Miller BR, Sanes JR, DiAntonio A. The requirement for Phr1 in CNS axon
760 tract formation reveals the corticostriatal boundary as a choice point for cortical axons.
761 Genes Dev. 2007;21(20):2593–606.
762 58. Culican SM, Bloom AJ, Weiner JA, DiAntonio A. Phr1 regulates retinogeniculate
763 targeting independent of activity and ephrin-A signalling. Mol Cell Neurosci [Internet].
764 2009;41(3):304–12. Available from: http://dx.doi.org/10.1016/j.mcn.2009.04.001
765 59. Vo BQ, Bloom AJ, Culican SM. Phr1 is required for proper retinocollicular targeting of
766 nasal-dorsal retinal ganglion cells. Vis Neurosci. 2011;28(2):175–81.
767 60. Wan HI, DiAntonio A, Fetter RD, Bergstrom K, Strauss R, Goodman CS. Highwire
768 regulates synaptic growth in Drosophila. Neuron. 2000;26(2):313–29.
769 61. Nakata K, Abrams B, Grill B, Goncharov A, Huang X, Chisholm AD, Jin Y. Regulation
770 of a DLK-1 and p38 MAP kinase pathway by the ubiquitin ligase RPM-1 is required for
771 presynaptic development. Cell. 2005;120(3):407–20.
772 62. Chuang K, Nguyen E, Sergeev Y, Badea TC Novel Heterotypic Rox Sites for Combinato-
773 rial Dre Recombination Strategies. G3 (Bethesda). 2015 Dec 29;6(3):559-71.
774
775
776
777
778 **FIGURE LEGENDS**

779 **Figure1: Cpne4 and Cpne4 dominant negative transfections in HEK293:** (A) Map of the
780 Flex construct. (B) Map of domain structure of Cpne4 shows three domains of the Cpne4
781 protein- two C2 domains (blue) and a vWA domain (purple). The location of the three Cpne4
782 plasmid constructs are shown by full length Cpne4 construct (orange), vWA domain construct
783 (brown) and C2 domains construct (green). The binding of the two Cpne4 antibodies- N-terminal
784 and C-terminal antibodies on the Cpne4 protein are indicated by yellow triangles. (C)
785 Representative images of HEK293 cells transfected with expression constructs for full length
786 Cpne4 (top row), C2 domains construct (middle row) and vWA domain construct (bottom row).
787 The cells were counterstained for eGFP (green), HA (red) and N-terminal or C-terminal Cpne4
788 (white) antibodies. Scale bar: 50um.
789
790 **Figure2: Cpne4 virus infections lead to 'bleb' formation on dendrites of Brn3b+ RGCs**
791 (A, B) Intraocular injections of AAV1-Cpne4 viruses were done in P0 or P14 Brn3b$^{Cre/WT}$ mice
792 eyes. Blebs were seen occasionally on dendrites of Cpne4 infected RGCs. For controls, AAV1-
793 eGFP was similarly injected in P0 Brn3b$^{Cre/WT}$ mice (C, D). No blebs were observed in the
794 control infected RGCs. Airy scan images for one of the blebs (A1) and adjoining dendrites (A2).
795 (E) Measurement of the 'bleb' areas for Cpne4 infected RGCs as compared to regular
796 varicosities on controls shows a significant difference between them while no difference between
797 P0 and P15 Cpne4 infected retinas. (F, G) Areas and lamination measurements indicate no
798 differences between the Cpne4 transfected RGCs as compared to control transfected RGCs. (ID:
799 inner distance- distance between outermost tip of RGC dendrites and the INL; IPL: width of the
800 IPL). Scale bar for A-C: 50um; Scale bar for A', A": 5um.
801

802 **Figure3: Yeast 2 hybrid analysis shows 5 proteins interacting with Cpne4 vWAdomain: (A)**
803 A Gal4 based yeast two hybrid analysis on the adult mouse retina cDNA library with Cpne4
804 vWA domain as bait protein showed five positive interactions (blue colonies). (B) Gel image of
805 colony PCR performed on the the positive clones from the yeast two hybrid shows the
806 corresponding interacting DNA sequences. The identity of these DNA sequences as confirmed
807 by the Sanger sequencing followed by BLAST analysis are shown as labels on the lanes. (C)
808 Sequences of some of the interacting peptides as identified by Sanger sequencing followed by
809 BLAST analysis are shown- HCFC1 (green); Mycbp2 (orange) and Morn2 (purple). The relative
810 positions of the actual interacting region on the respective protein is indicated by arrows and any
811 protein domains in that region and surrounding regions are also labeled.
812
813 **Figure4: Cpne4 Adomain was pulled down with HCFC1, Morn2 and Mycbp2, but not by**
814 **Tox3:** (A) Map of a Flag clone consisting of a Flag tag followed by the interacting regions of
815 HCFC1, Morn2, Mycbp2 and Tox3. (B-E) Representative images of HEK293 cells co-infected
816 with the expression construct for Cpne4vWAdomain (HA-Cpne4vWA) and Flag- tagged
817 interacting protein. (F, G) Box plots and violin plots indicate the Spearmann's correlation
818 coefficient for cololcalization between Morn2, HCFC1, Tox3 or Mycbp2 with Cpne4. (H)
819 Western blot images of pull down from co-transfected HEK293 cells using Flag antibody show
820 the total lysate (*I*) and the co-immunoprecipitated (*C*) proteins. Cpne4-vWA (green; 31kDa)
821 pulled down Flag- HCFC1 (23.5kDa), Morn2 (21kDa), Mycbp2 (42kDa) and not Tox3 (66kDa).
822 Scale bar: 50um.
823

824 **Figure5: Expression of Morn2, HCFC1 and Mycbp2 in retina:** (A) RNA sequencing data for
825 Morn2, Mycbp2 and HCFC1 in different brain areas, Brn3a WT and KO RGCs, Brn3b WT and
826 KO RGCs and rest of the retina. (B) HCFC1 (red) immunostaining in retina indicates some
827 expression in RGCs in both the WT and Brn3b KO retinas. There is some co-labeling with
828 Cpne4 (green) in the RGC cell bodies (arrows). (C) Morn2 (green) immunolabeling in the retina
829 indicated mostly dendritic labeling in the IPL in both Brn3b WT and KO retinas. There is also
830 some Morn2 labeling in the OPL of WT that is reduced in the Brn3b KO. Scale bar: 50um.
831
832 **Figure6: Pulldown with GST-Cpne4 or GST-CpneAdomain and LC-MS:** (A) Representative
833 SDS-PAGE gel for retina pull downs using GST- Cpne4, GST- Cpne4- vWA and GST only
834 (n=3). (B) Representative Western blot image of some of the interactors from the pull down
835 experiment- pan 14-3-3 (30kDa); Map1b (325kDa); SV2 (95kDa) and Syntaxin1 (33kDa) as
836 compared to GST (28kDa) control. (C) Volcano plot for proteins that had a significant
837 interaction with GST- Cpne4 as compared to GST control. (D) Volcano plot for proteins that had
838 a significant interaction with GST- Cpne4- vWA as compared to GST control.
839
840 **Figure7: Immunostaining of LC-MS interactors with Cpne4 in retina:** Representative
841 images showing immunostaining of pan 14-3-3 (A); Map1b (B); SV2 (C) and Syntaxin (D; red)
842 with Brn3b (green) in Brn3b WT (left panel) and KO (right panel). Scale bar: 50um.
843
844
845 **Table1:** List of antibodies used for immunofluorescence and WB
846

Antigen	immunogen	Antibody details	Dilution used for IHC (and WB)
C- terminal Cpne4	EVYESSRTLA	made in house, rabbit polyclonal	1:2000 (1:1000 for WB)
Brn3a	Human Brn3a aa186–224 protein 10 fusion (pGEMEX)	Millipore, mouse monoclonal, Cat# MAB1585	1:20
Brn3b	Human Brn3b aa184–252 GST fusion	made in house, rabbit polyclonal	1:20
mouse HA	CYPYDVPDYASL	Covance, mouse monoclonal, clone 16B12	1:100
rabbit HA	YPYDVPDYASL	Cell Signaling Technologies, rabbit polyclonal, Cat# 3724	1:100
GFP	Recombinant full length GFP	Abcam, chicken polyclonal, Cat# ab13970	1:700

Morn2	Recombinant protein against the epitope- MNGFGRLEHFSGAVYEGQFK DNMFHGLGTYTFPNGAKYT G NFNENRVEGEGEYTDIQGLE WS GNFHFTAAPDLKLK	Sigma prestige antibodies, rabbit polyclonal, Cat# HPA057815	1:100
HCF1	aa 206-251 mapping near the N-terminus of human HCF1	Santa Cruz Biotechnology, mouse monoclonal, Cat# sc-390950	1:50
Map1b	aa 6-31 at the N-terminus of human MAP-1B	Santa Cruz Biotechnology, mouse monoclonal, Cat# sc-365668	1:50 (1:250)
Pan 14-3-3	aa 1-30 at the N-terminus of human pan 14-3-3	Santa Cruz Biotechnology, mouse monoclonal, Cat# sc-1657	1:50 (1:500)

SV2	Purified synaptic vesicles	Developmental Studies Hybridoma Bank, DSHB, of the University of Iowa, USA, mouse monoclonal	1:500 (1:2000)
Syntaxin1	Recombinant protein corresponding to AA 1 to 262 from rat Syntaxin1A (UniProt Id: P32851)	Synaptic systems, mouse monoclonal, Cat# 110011	1:200 (1:2500)
GST	26 kDa GST specific domain of a fusion protein encoded by a pGEX.3X recombinant vector	Santa Cruz Biotechnology, rabbit polyclonal, Cat# sc-459	(1:750)

847

848

849

850

851

852

853

854

855

856

857

858

859

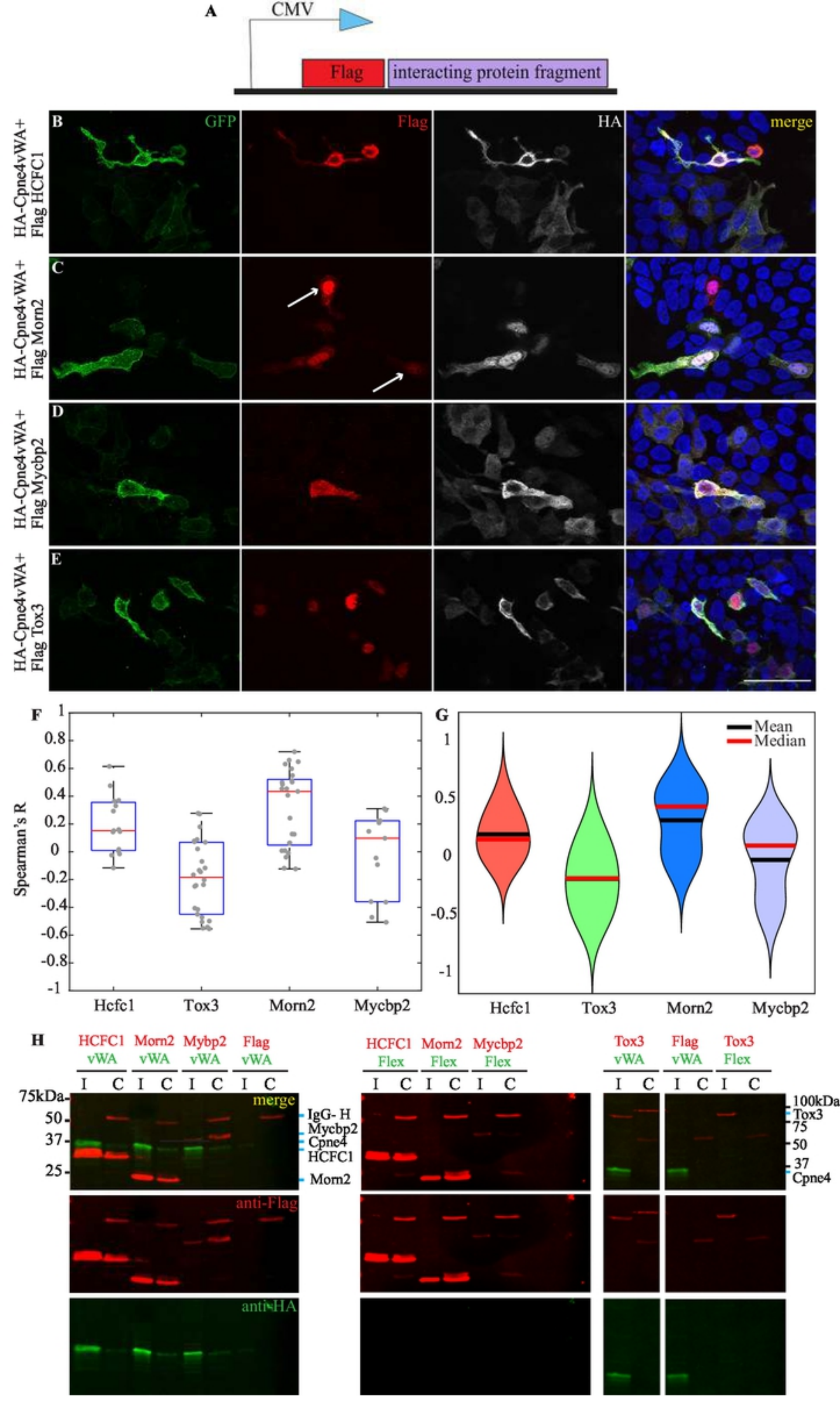
A
CMV
Flag
interacting protein fragment
B
GFP
Flag
HA
merge
HA-Cpne4vWA+
Flag HCFC1
C
HA-Cpne4vWA+
Flag Morn2
D
HA-Cpne4vWA+
Flag Mycbp2
E
HA-Cpne4vWA+
Flag Tox3
F
Spearman's R
Hcfc1
Tox3
Morn2
Mycbp2
G
Mean
Median
Hcfc1
Tox3
Morn2
Mycbp2
H
HCFC1 vWA
Morn2 vWA
Mybp2 vWA
Flag vWA
HCFC1 Flex
Morn2 Flex
Mycbp2 Flex
Tox3 vWA
Flag vWA
Tox3 Flex
I C
75kDa
50
37
25
merge
IgG- H
Mycbp2
Cpne4
HCFC1
Morn2
anti-Flag
anti-HA
100kDa
Tox3
75
50
37
Cpne4

Figure 4

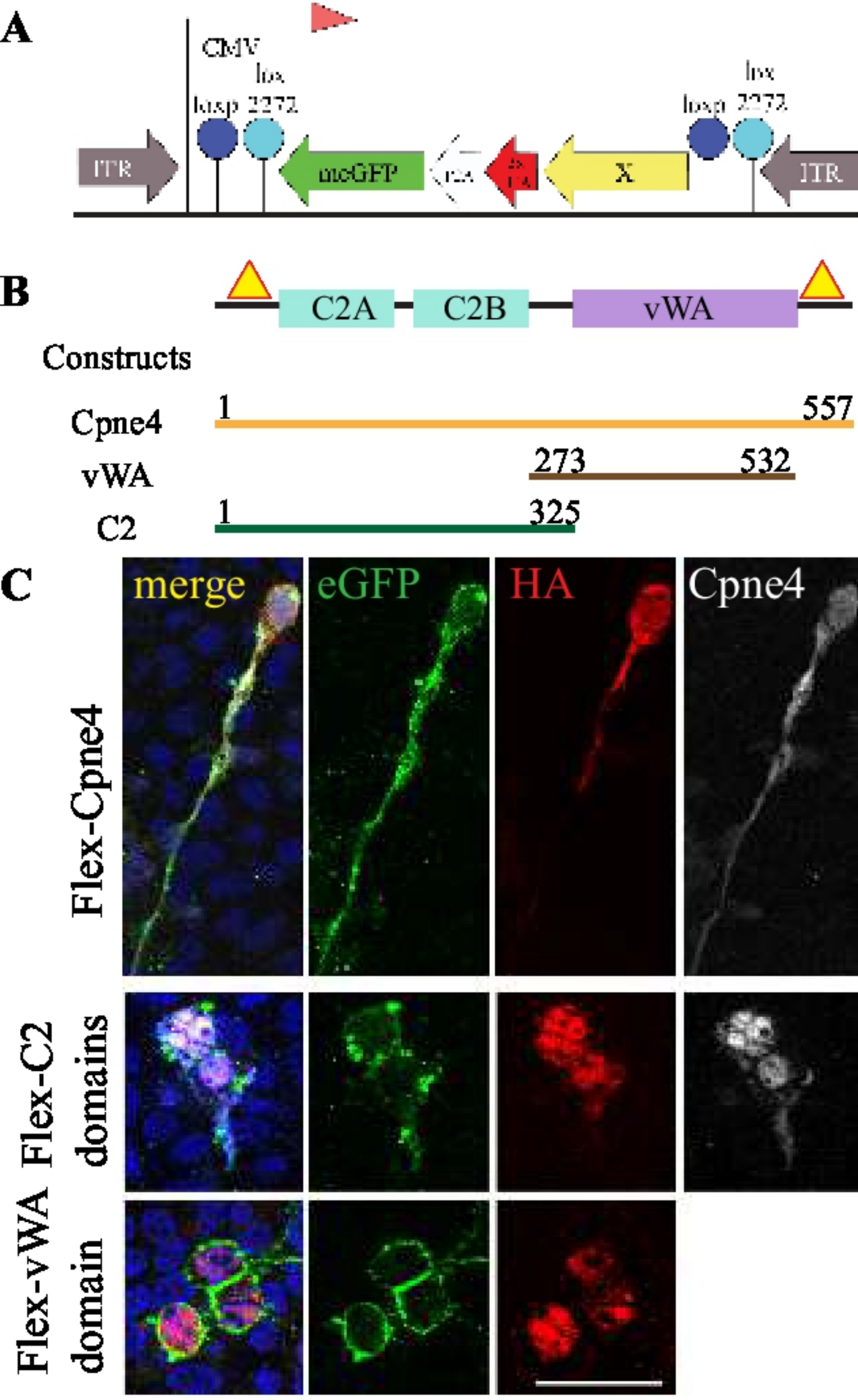
A
CMV
lox
loxp 2272
lox
loxp 2272
ITR
mcGFP
r2A
X
ITR
B
C2A
C2B
vWA
Constructs
Cpne4
1
557
vWA
273
532
C2
1
325
C
merge
eGFP
HA
Cpne4
Flex-Cpne4
Flex-C2 domains
Flex-vWA domain

Figure 1

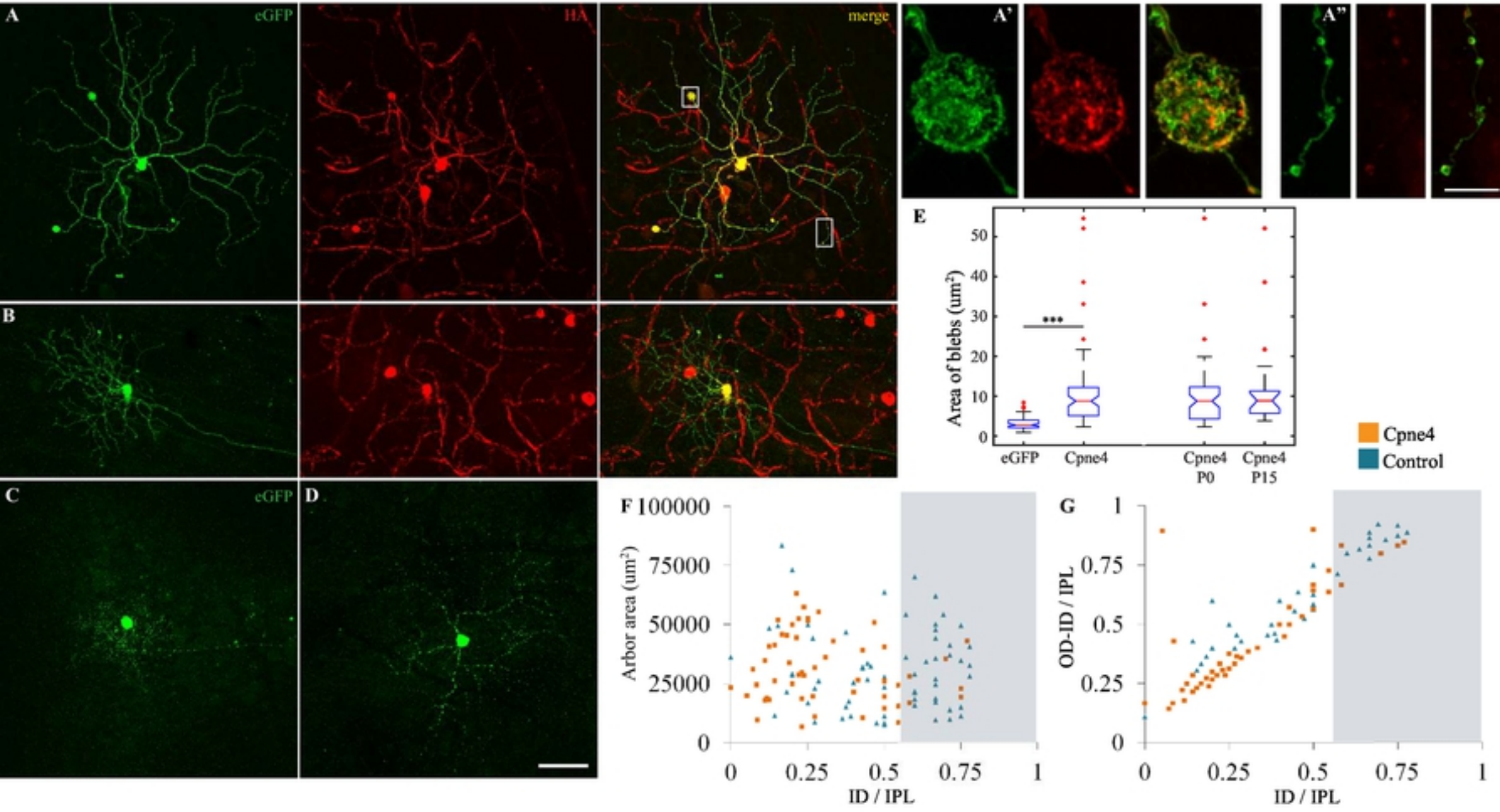
A
eGFP
HA
merge
A'
A''
B
C
eGFP
D
E
Area of blebs (um²)
***
eGFP
Cpne4
Cpne4 P0
Cpne4 P15
Cpne4
Control
F
Arbor area (um²)
ID / IPL
G
OD-ID / IPL
ID / IPL

Figure 2

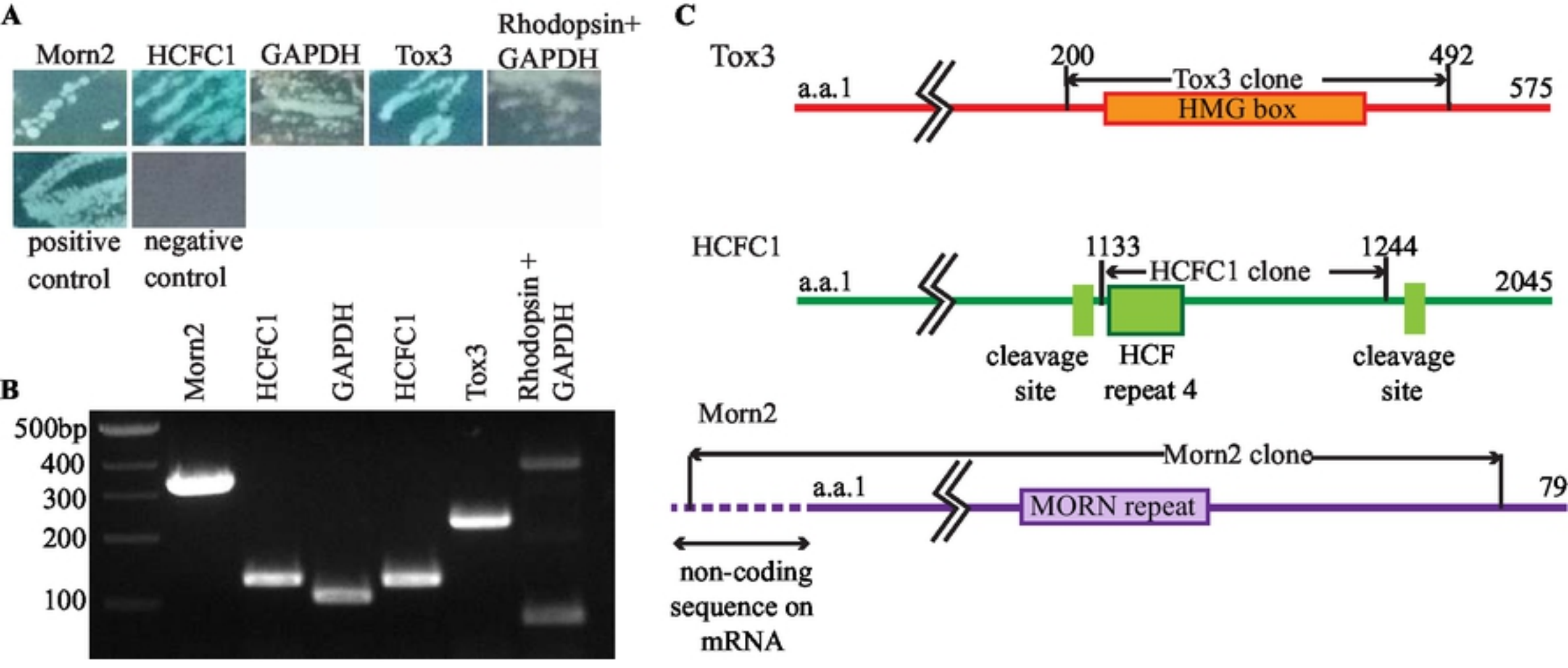
A
Morn2
HCFC1
GAPDH
Tox3
Rhodopsin+ GAPDH
positive control
negative control
B
Morn2
HCFC1
GAPDH
HCFC1
Tox3
Rhodopsin + GAPDH
500bp
400
300
200
100
C
Tox3
a.a.1
200
492
Tox3 clone
HMG box
575
HCFC1
a.a.1
1133
1244
HCFC1 clone
2045
cleavage site
HCF repeat 4
cleavage site
Morn2
Morn2 clone
a.a.1
MORN repeat
79
non-coding sequence on mRNA

Figure 3

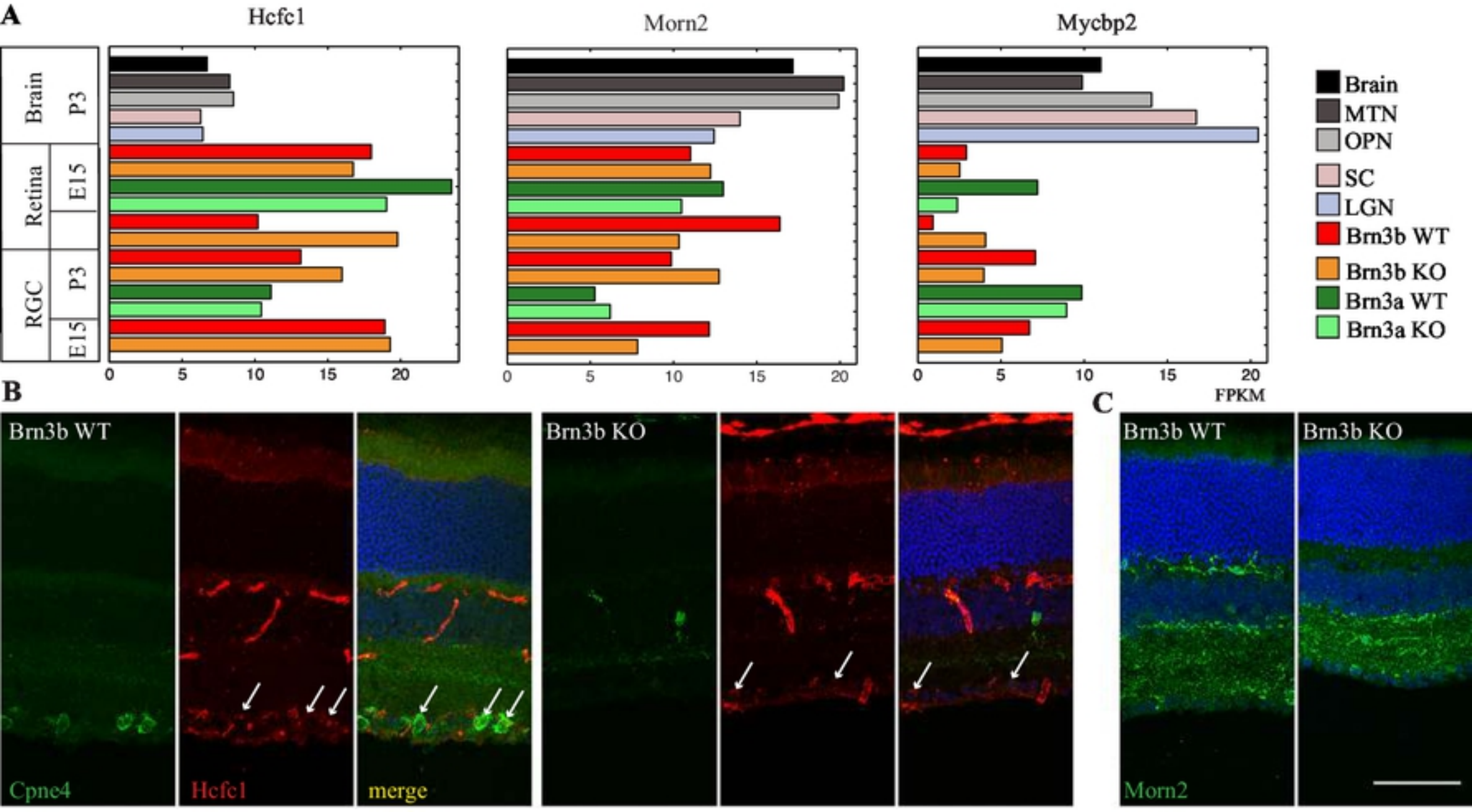
A
Hcfc1
Morn2
Mycbp2
Brain
P3
Retina
E15
RGC
P3
E15
0
5
10
15
20
FPKM
Brain
MTN
OPN
SC
LGN
Brn3b WT
Brn3b KO
Brn3a WT
Brn3a KO
B
Brn3b WT
Brn3b KO
Cpne4
Hcfc1
merge
C
Brn3b WT
Brn3b KO
Morn2

Figure 5

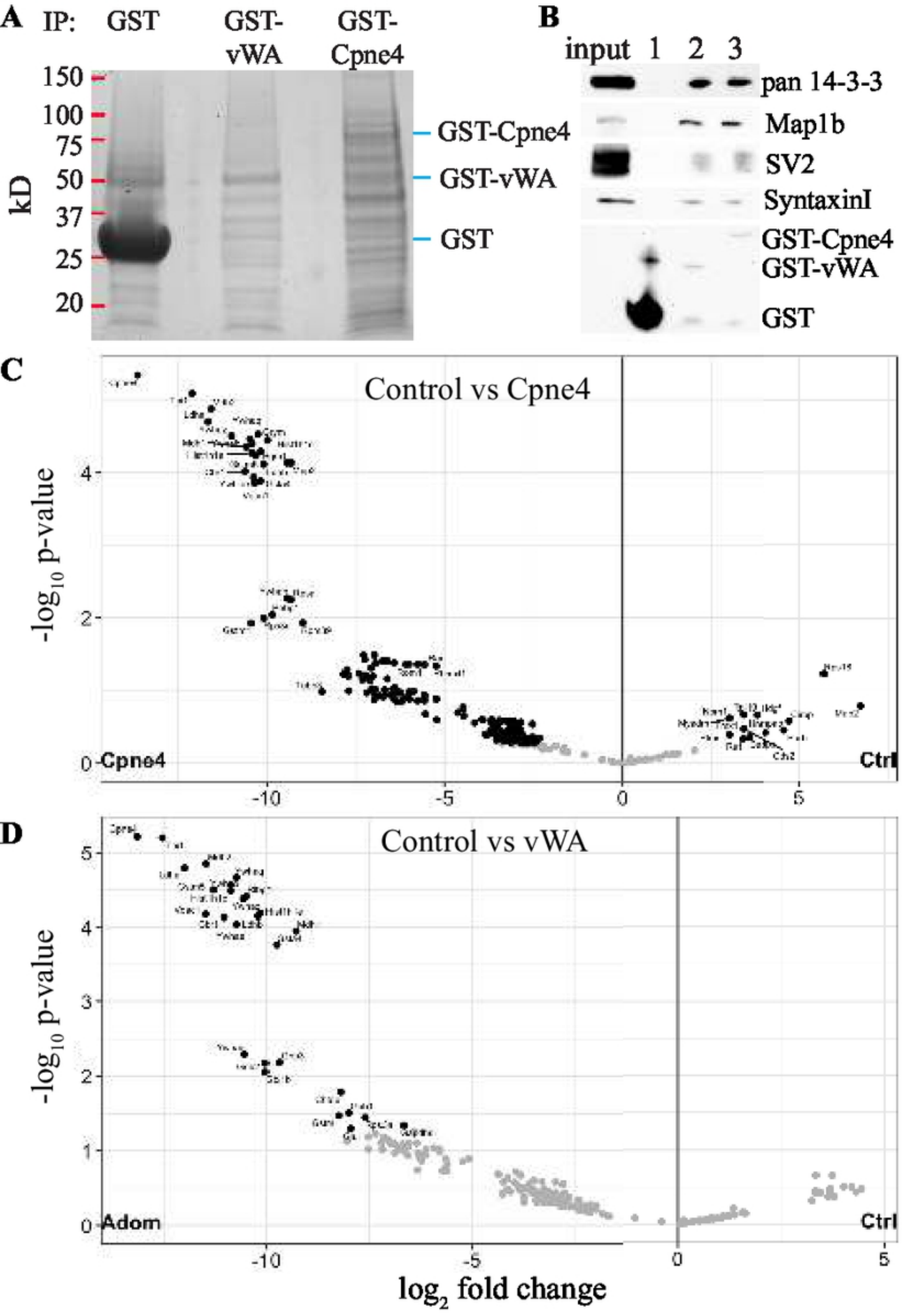
A
IP: GST
GST-vWA
GST-Cpne4
150
100
75
50
37
25
20
kD
GST-Cpne4
GST-vWA
GST
B
input 1 2 3
pan 14-3-3
Map1b
SV2
SyntaxinI
GST-Cpne4
GST-vWA
GST
C
Control vs Cpne4
-log10 p-value
Cpne4
Ctrl
D
Control vs vWA
Adom
Ctrl
log2 fold change

Figure 6

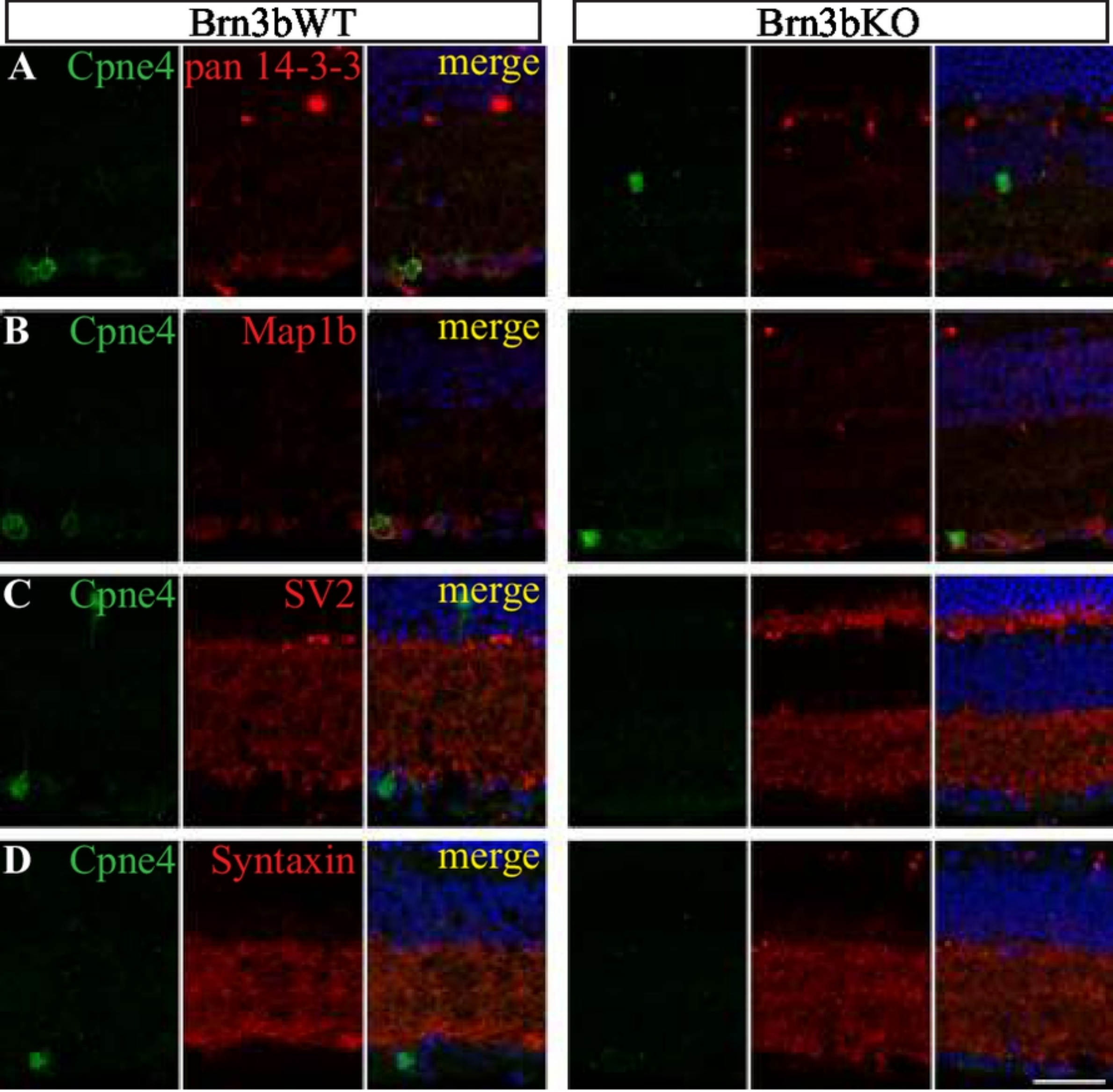
Brn3bWT
Brn3bKO
A
Cpne4
pan 14-3-3
merge
B
Cpne4
Map1b
merge
C
Cpne4
SV2
merge
D
Cpne4
Syntaxin
merge

Figure 7